Numerical Investigation on the Initial Development of Layered Coal Dust Combustion

Kei Shimura and Akiko Matsuo

Department of Mechanical Engineering, Keio University
3-14-1 Hiyoshi, Kohoku-ku, Yokohama, Kanagawa 223-8522, Japan

1 Introduction

Dust explosions are rapid combustion of dispersed dust suspended in air. Solid particles are usually unreactive because they are layered on the bottom due to gravitational effects. In many cases, primary explosion caused by electrical spark or frictional heat is a trigger of dust explosion, and layered dust is dispersed into air. The studies on understanding dust explosions have two topics: dispersed dust explosion and layered dust explosion. Dispersed dust explosion is the flame passing through dispersed dust cloud and often appears in powder process industry. The flame of dispersed dust combustion easily propagates after ignition and causes severe accidents to industrial facilities. In addition, supersonic propagation appears in closed combustion. Many previous studies were performed to clarify explosion limits such as concentration and ignition energy. Layered dust explosion is the flame propagated over dust layer and possibly occurs at more wide industries such as woodworking. Layered dust combustion behaves different from dispersed dust combustion and can also cause supersonic propagation of the flame. Theoretical and experimental researches have been performed to understand the layered dust explosions. However, there are difficulties in visualization for complicated processes including the shock propagation, the dust lifting, and the combustion of non-premixed devolatilized gas. Numerical analysis of fully developed layered coal dust detonation was performed to focus on detonation structure with transverse waves[1]. Their simulations were based on Euler-Euler approach, which treats particle phase with continuous assumption.

The purpose of this study is to understand mechanism of initial development of layered coal dust combustion by using numerical simulation, where Particle-In-Cell method[2] with parcel assumption is employed to explain the dispersed particle behavior.

2 Numerical Method

The numerical model for coal-dust combustion is based on two-fluid model and volume fractions of each phase are introduced for set of equations. Governing equations for gas phase are balance equations for mass, momentum, energy, and mass fraction for each species with porosity. Gas phase is presumed to

Correspondence to: shimura@mech.keio.ac.jp (K. Shimura)

compressible viscous fluid and consists of 6 species (CH_4, O_2, N_2, CO, CO_2, H_2O). Each equation includes source term for interaction with particle phase and homogeneous gas reaction. Thermally perfect gas assumption and ideal equation of state are applied to close the set of equations. NASA polynomial function with CETPC table[3] is applied to estimate heat capacity and enthalpy.

Particle phase is regarded as incompressible inviscid fluid. We applied Particle-In-Cell method to deal dispersed particle behavior. In this method, particle phase is treated by continuum approach and discontinuum approach. The balance equation of the solid phase for momentum is calculated from continuum side to estimate particle velocity on the grid system. Solid momentum equation includes source term of phase interaction and particle-particle interaction force estimated by Andrews internal force equation[2]. In the discontinuum side, we calculate balance of mass, energy, angular momentum, and mass fractions on Lagrangian coordinate for each parcel. Particle phase consists of 3 species (CH4, C, Ash).

Drag force, Magnus lift force, and Saffman force are treated for interphase momentum transfer. Each force is calculated by Gidaspow model[4], Rubinow model[5], and Saffman model[6], respectively. Thermal conduction is simulated to deal energy transfer and local heat transfer coefficient is estimated by Ranz-Marshall equation[7].

The chemical reaction of coal particles consists of heterogeneous reaction and homogeneous reaction. The devolatilization of methane and combustion of fixed carbon are considered for heterogeneous reactions. Their reaction rates are given as Badzioch et al. (1970)[8] and Field's model[9]. The homogeneous reaction after devolatilization and gasification are presumed to be two-step irreversible global reactions given by Semenov et al.(2013)[1].

The discretization methods are 3rd-order SHUS[10] for convection term and 2nd-order central difference for viscous term. Time integration methods are MTS method[11] for chemical reaction term and 3-step Runge-Kutta for the other terms.

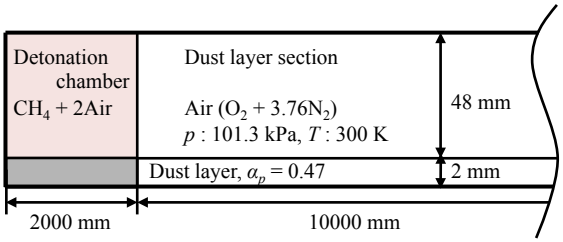

Fig. 1. Schematic of computational target

3 Result and Discussion

Figure 1 illustrates a numerical target to discuss initial development of layered coal dust combustion. The calculation domain is 12 m long channel with height of 50 mm. The domain consists of detonation chamber of 2 m length and dust layer section filled with pure air at 101.3 kPa and 300 K. The detonation chamber contains stoichiometric CH_4-Air mixture at 101.3 kPa and 300 K, and the heat source at 1013 kPa and 1000 K is set to initiate gas detonation. Coal particles are placed uniformly from the tube base to the height of 2 mm in the dust layer section, where the volume fraction of particle phase is 0.53. The coal dust particles are assumed to be Huolinhe particles[12]. An outlet condition is utilized for the right end, and an adiabatic wall condition is applied for the other boundaries. The computational grid is square with $\Delta x = \Delta y = 500$ μm, and the number of parcels is 40000x8. Initially,

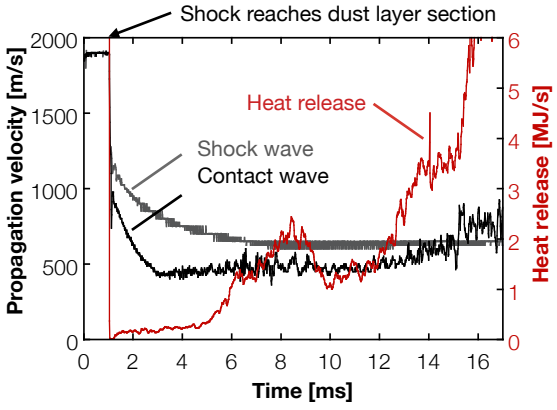

Fig. 2. Time histories of propagation velocities of the shock wave and the contact wave, and heat release rate of homogeneous chemical reaction

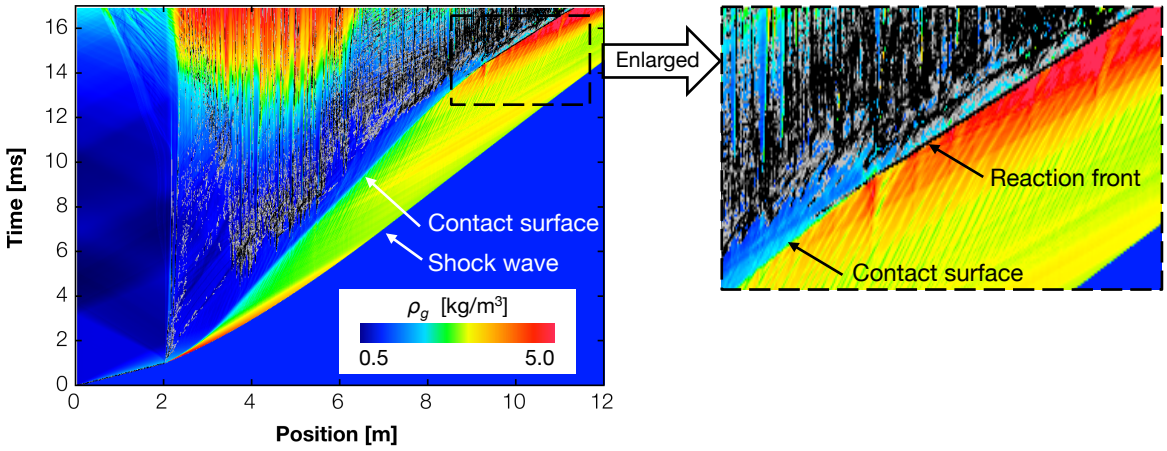

Fig. 3. The x-t diagram of cross-sectional averaged gas density (color counter) and higher heat release rate q > 10^7 J (black line)

gas detonation wave propagates in the detonation chamber and penetrates into the dust layer section. The detonation wave is quenched due to absent of combustible gas in the dust layer section, and strong shock wave and high-temperature detonation products interact with layered coal-dust. Then, dust particles are lifted by the shock wave and ignited by the interaction of high-temperature gas.

Time histories of propagation velocities of the shock wave and the contact surface, and the rate of energy release by homogeneous chemical reaction are shown in Fig. 2. The contact surface means the contact between detonation products and ambient air in the dust layer section. The propagation velocities of shock wave and contact surface are over 1500 m/s until 1 ms because gas detonation propagates in the detonation chamber. After 1 ms, the velocities dramatically decrease due to the lack of combustible gas and the contact surface propagates at 500 m/s. The shock wave propagation becomes stable with the velocity of 600 m/s after 7 ms. There are three noticeable jumps of the heat release rate at 6, 12, 15 ms. The first jump is due to the initiation of dust combustion by the interaction between particles and detonation products. The final jump causes the acceleration of the contact surface. The propagation velocity of contact surface exceeds the shock velocity after 15 ms, and deflagration to detonation may occur by the significant heat release.

The trajectories of shock wave and contact surface are indicated in Fig. 3, and black line shows the regions of higher heat release rate ($q > 10^7$ J). The contact surface (reaction front) is decoupled with the shock wave at x = 2 m and accelerates at x = 9 m. After 15 ms, the homogeneous chemical reaction appears at the contact surface and newly reaction front is formed as indicated in enlarged view. The higher density region appears at x = 2 – 6 m after 12 ms. No chemical reaction appears at this region, so that the reason why the gas density increases is devolatilization. The distance between the contact surface and the higher density region indicates ignition delay time of coal dust.

Figure 4 shows the x-t diagram for cross-sectional averaged pressure and gas velocity. The higher pressure region between 2 and 6 m agrees with the high density region. It indicates that the devolatilization directly affects pressure field due to the narrow channel of calculation domain. In the horizontal velocity distribution, the gas velocity is accelerated by the pressure gradient and exceeds the flame propagation velocity (600 m/s in Fig. 2) after 14 ms. In addition, the accelerated gas decelerates on the contact surface. These results suggest that the contact surface or reaction front is accelerated by the gas flow behind the flame. Also, devolatilization further behind the flame supports the flame acceleration.

Figure 5 shows the distributions of gas temperature, CH_4 mass fraction, O_2 mass fraction, energy release rate of homogeneous reaction, and gas horizontal velocity at 14.5 ms and 15.5 ms. 14.5 ms and 15.5 ms represents before and after the acceleration indicated in Fig. 2. The right tip of high temperature region appears in front of the right tip of CH_4 rich region as shown in Fig. 5(a). Almost all devolatilized CH_4 in the channel has no reaction due to lack of ambient O_2. Only lower surface of high temperature region can cause chemical reaction because of presence of O_2 inside the dust layer. The gap between right tip positions of temperature and CH_4 region is filled with the detonation products because this region has no devolatilized CH_4 and ambient O_2. These detonation products are generated by initial gas detonation to initiate the dust combustion.

The devolatilized CH_4 catches up the right tip of high-temperature region as shows in Fig. 5(b). The reaction of CH_4 at the upper area appears due to the contact with ambient air. Therefore, the increase of energy release rate at 15 ms as shown in Fig. 2 is the beginning of CH_4 combustion at the right tip. It is considered that the flame in this circumstance is diffusion flame because the flame is generated on the contact surface between ambient air and devolatilized gas. The flame propagation velocity (the advection velocity of diffusion flame) is determined by the advection of devolatilized gas.

Figure 6 shows the schematic of flame acceleration mechanism based on the previous observations of Fig. 5(b). The calculated flame is essentially diffusion flame and the reaction front appears at the contact surface between ambient air and devolatilized CH_4. The advection of this diffusion flame is supported by the advection of CH_4.

The sequence of the flame acceleration is summarized. First, gas temperature increases at the reaction front and dust particles are heated and ignited. Due to the ignition delay and characteristic time of thermal transfer, the devolatilization of coal-dust mainly occurs 3 m behind the reaction front and CH_4 gas spreads. Then, pressure and gas density dramatically increase by the mass transfer effects, and pressure gradient is generated. Homogeneous chemical reaction of CH_4 does not occur further behind the reaction front because of the lack of O_2. However the gas further behind the reaction front is accelerated to 1000 m/s by the pressure gradient and their velocity exceeds the reaction front advection velocity (600 m/s). Finally, CH_4-rich mixture behind the flame can catch up the reaction front. The diffusion flame moves rightward, which looks like "propagates" by supplying fuel from behind. Although fixed carbon combustion of dust particles is calculated in this simulation, no heterogeneous combustion appears behind the reaction front due to the lack of O_2. This is because the reaction front consumes almost of all O_2. On the other hands, devolatilization has sufficient effects for the propagation of the flame because of no requirement of oxidant for phase transition.

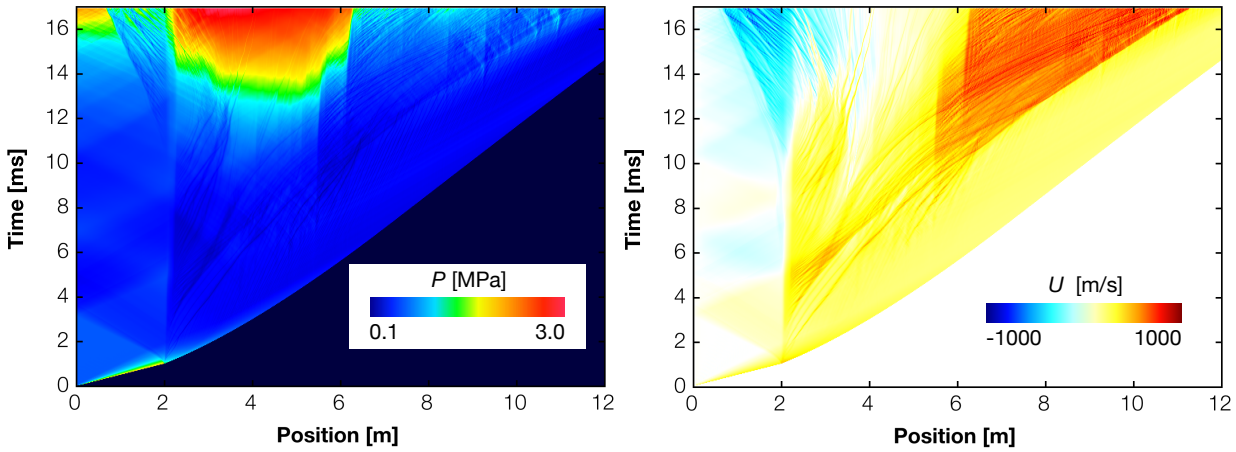

Fig. 4. The x-t diagram of cross-sectional averaged pressure and gas horizontal velocity

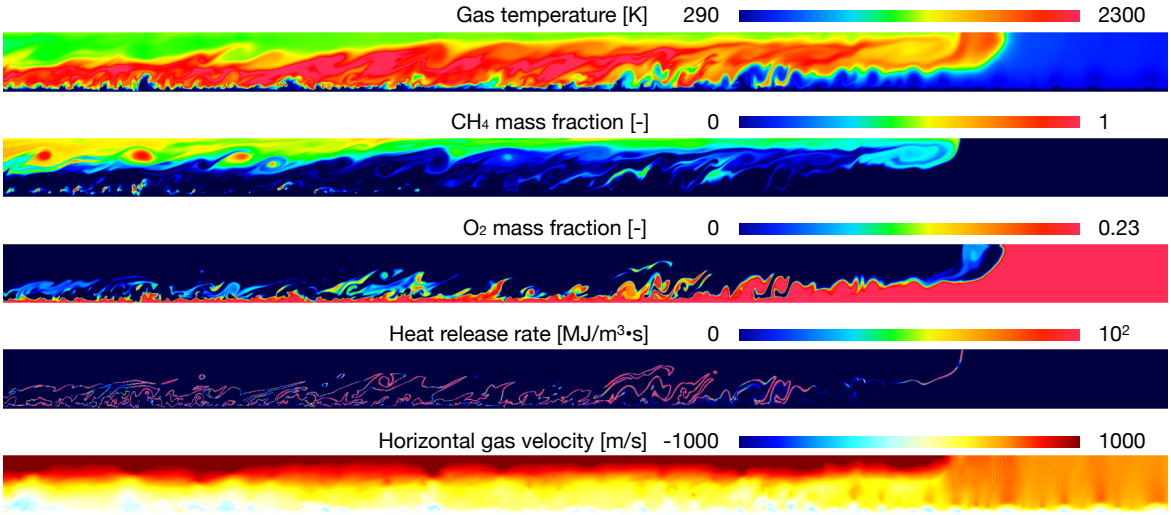

(a) 14.5 ms, before flame acceleration

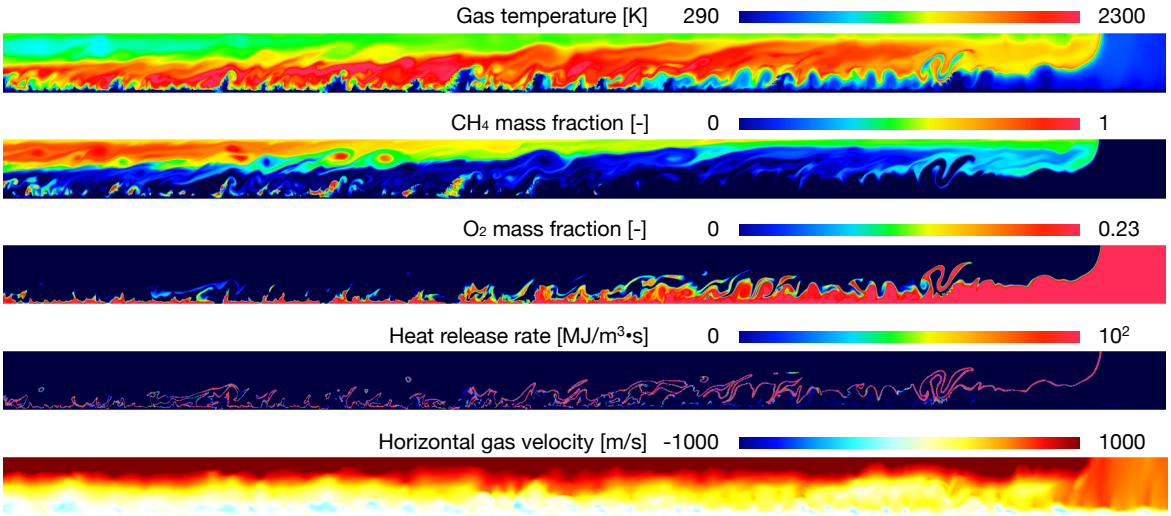

(b) 15.5 ms, after flame acceleration

Fig. 5. The distributions of gas phase quantity before and after flame acceleration

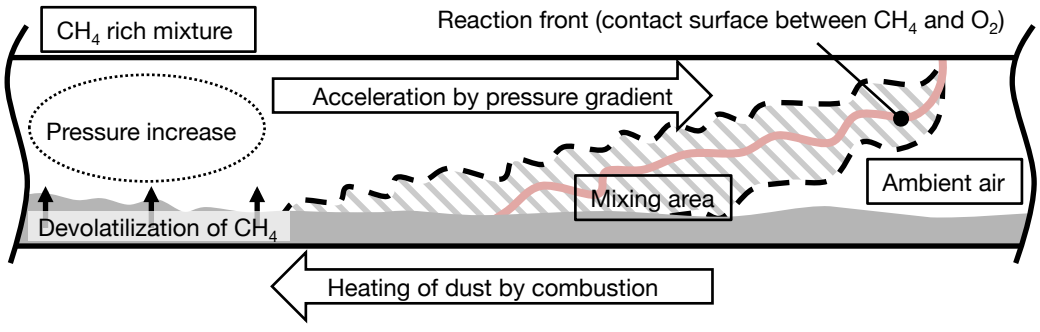

Fig. 6. Schematic illustration of flame advection mechanism for initial stage of layered dust combustion

4 Conclusions

In this study, the flame acceleration mechanism of layered dust combustion is numerically investigated. The activation of devolatilization 3 m behind the reaction front causes the flame acceleration. The density increase of gas phase generates the pressure gradient, and the devolatilized CH_4 is accelerated by this gradient. Accelerated CH_4 catches up the reaction front and the flame velocity exceeds the shock propagation velocity. The flame advection is supported by three phenomena, thermal transfer from the reaction front to dust particles, pressure and density increases by devolatilization, and acceleration of devolatilized CH_4 by the pressure gradient.

References

[1] Semenov I, Utkin P, Markov V. (2013). Numerical modelling of dust-layered detonation structure in a narrow tube. J. Loss Prev. Process Ind. 26: 380.

[2] Andrews MJ, O'Rourke PJ. (1996). The multiphase particle-in-cell (MP-PIC) method for dense particulate flow. Int. J. Multiphase Flow 22: 379.

[3] McBride BJ, Gordon S, Reno MA. (1993). Coefficient for calculating thermodynamic and transport properties of individual species. NASA Technical Memorandum 4513: 10.

[4] Gidaspow D. (1994). Multiphase Flow and Fluidization: Continuum and Kinetic Theory Descriptions. Academic Press (ISBN 9780080512266).

[5] Rubinow SI, Keller JB. (1961). The transverse force on a spinning sphere moving in a viscous fluid. J. Fluid Mech. 101: 257.

[6] Saffman P. (1965). The lift on a small sphere in a slow shear flow. J. Fluid Mech. 22: 385.

[7] Ranz WE, Marchall WR. (1952). Evaporation from drops. Chem. Eng. Prog. 48: 141.

[8] Badzioch S, Hawksley GW. (1970). Kinetics of thermal decomposition of pulverized coal particles. Ind. Eng. Chem. Process Des. Dev. 9: 521.

[9] Field MA. (1969). Rate of combustion of size-graded fractions of char from low-rank coal between 1200 K and 2000 K. Combust. Flame 13: 237.

[10] Shima E, Tadamasa J. (1997). Role of CFD in aeronautical engineering (No.14) -AUSM type upwind schemes. Proc. 14th NAL Symp. Aircraft Comput. Aerodynamics.

[11] Gou X, Sun W, Chen Z, Ju Y. (2010). A dynamic multi-timescale method for combustion modeling with detailed and reduced chemical kinetic mechanisms. Combust. Flame 157: 1111.

[12] Cao W, Gao W, Peng Y, Liang J, Pan F, Xu S. (2014). Experimental and numerical study on flame propagation behaviors in coal dust explosions. Powder Technol. 266: 456.